Femtosecond Stokes shift in styryl dyes: Solvation or intramolecular relaxation?

S. A. Kovalenko, N. P. Ernsting, and J. Ruthmann

Citation: The Journal of Chemical Physics **106**, 3504 (1997); doi: 10.1063/1.473447
View online: http://dx.doi.org/10.1063/1.473447
View Table of Contents: http://scitation.aip.org/content/aip/journal/jcp/106/9?ver=pdfcov
Published by the AIP Publishing

Femtosecond Stokes shift in styryl dyes: Solvation or intramolecular relaxation?

S. A. Kovalenko[a)]
Max-Planck-Institut für Biophysikalische Chemie, D-37018 Göttingen, Germany

N. P. Ernsting[b)]
Institut für Physikalische und Theoretische Chemie der Humboldt-Universität, Bunsenstrasse 1, D-10117 Berlin, Germany

J. Ruthmann
Max-Planck-Institut für Biophysikalische Chemie, D-37018 Göttingen, Germany

(Received 17 April 1996; accepted 21 November 1996)

Transient absorption and gain spectra of the styryl dye LDS-750 in solution have been studied by the pump/supercontinuum probe (PSCP) technique with excitation at 530 nm. The pump/probe intensity correlation width was 70 fs, providing a time resolution of 40 fs. Spectra were detected in the range 400–800 nm with 1.5 nm resolution. Before 70 fs, prominent spectral structure is observed due to resonant Raman scattering from a 1500 cm^{-1} active mode of the chromophore. At later time, the gain spectrum undergoes an ultrafast redshift and change of shape, with time constants of ~200 and ~600 fs for acetonitrile and chloroform solutions, respectively. At high pumping energy (1.2 μJ), the final emitting state is reached by internal conversion from higher electronic states without a further essential Stokes shift. The emitting state is assigned to an excited isomeric form of the molecule. At low pumping energy (0.3 μJ), the first excited electronic state isomerizes in an ultrafast process followed by a slower process, the dynamics of which is controlled by the solvent. The geometrical and electronic nature of these processes and their coupling to the solvent needs further clarification. © *1997 American Institute of Physics.* [S0021-9606(97)02908-5]

I. INTRODUCTION

Femtosecond solvation dynamics in polar liquids has proved an attractive and fascinating challenge for theoreticians and experimentalists alike. The reason is that ultrafast solvation may control the dynamics of charge transfer and other condensed-phase chemical reactions.[1] Both molecular dynamics simulations[2–4] and quasianalytical approaches[5,6] predict the existence of an ultrafast (inertial) component of solvation on a time scale below 100 fs. The first experimental observation of this component, by fluorescence upconversion, was reported in Ref. 7(a) for the styryl dye LDS-750 (=Styryl 7, see inset in Fig. 1) in acetonitrile. Later, other workers obtained similar results for different solvatochromic molecular probes in a variety of solvents from transient fluorescence,[8–11] dynamical hole burning,[12] and photon echo[13–15] measurements. The dominance of ultrafast solvation for the initial time regime was generally assumed. However, *intra*molecular processes in a probe molecule, like vibrational relaxation or ultrafast isomerization due to vibronic coupling of neighboring electronic states, may contribute to the transient signal. For any solvatochromic probe there remains the task of recognizing intramolecular contributions and of separating them from solvation dynamics.

This is particularly necessary for styryl dyes which may isomerize in the excited state along multidimensional paths which are still not completely identified. LDS-750[7,16,17] provides a case in point. Figure 1 shows its stationary optical spectra (solid lines) in acetonitrile. Here, the fluorescence intensity was converted into cross sections for stimulated emission for comparison with the transient spectra. The stationary emission band has a width (FWHM) of 1490 cm^{-1} while the absorption band is 4600 cm^{-1} wide. This deviation from mirror symmetry has been noted before[16] and led to concern about the use of styryl dyes as solvatochromic probes.[9(a),17] It indicates that more than one electronic state is involved in the absorption region and/or that the equilibrium geometry and normal coordinates of the optically excited state differ from those of the emitting state.

To develop this point further, we seek additional information about active normal modes and the shape of the transient emission spectra. Here, we report new results from a study of LDS-750 in acetonitrile and chloroform which show that an intramolecular process dominates the observed Stokes shift. We applied the pump/supercontinuum probe (PSCP) technique for studying transient optical gain and absorption spectra of the dye solution. It is a characteristic feature of this technique that spectral and temporal resolution are equally stressed and that details of the spectral evolution are readily recognized.[18]

II. EXPERIMENT

LDS-750 was used as received from Exciton Chemicals. The experimental setup is essentially the same as in Ref. 18 and has been described elsewhere.[12] The basic pulses at 530 nm (repetition rate 2 Hz) are compressed to ≈45 fs with pulse energy of 60 μJ. This beam is split in two parts. The

[a)]On leave from the Institute of Chemical Physics, Russian Academy of Sciences, Moscow 117977.
[b)]To whom correspondence should be addressed.

 0021-9606/97/106(9)/3504/8/$10.00

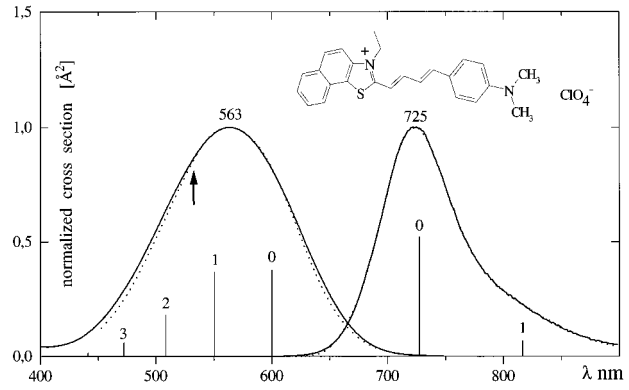

FIG. 1. Steady-state absorption and emission spectra of LDS-750 in acetonitrile at 22 °C. Vertical lines indicate Franck–Condon factors which were used for the simulated absorption and emission spectra (see the text).

first part, after passing a variable delay stage, is used for optical pumping. The pump beam has a diameter of 150 μm on the sample with a typical pulse energy of 0.3 μJ. The second part ($\sim$10 μJ) is focused into a fused silica plate (2 mm) to generate a supercontinuum probe which is imaged onto the pumped sample region to a diameter of 90–100 μm. Pump and probe beams intersect at an angle of 5°. The sample thickness is 0.3 mm, and the solution is flown out of the laser region after each shot. The concentration of the dye in solution ($\sim 3\cdot 10^{-4}$ molar) is adjusted to give an optical density OD$\approx$0.4 at the pump wavelength. The intensity autocorrelation of the pump pulses—measured in the same geometry—has FWHM of 64–70 fs corresponding to pulses shorter than 50 fs. The spectral width of the pump pulses is 12 nm (430 cm^{-1}).

After interaction with the sample, the supercontinuum probe pulse is dispersed by a polychromator and registered on a photodiode array (512 pixels covering 400–800 nm). Changes of optical density, ΔOD, as a function of probe wavelength λ are calculated by comparison with a simultaneously recorded reference spectrum. Typically eight measurements are averaged to give a transient spectrum at every time step of 6.7 fs. Because the supercontinuum is chirped, the recorded $\Delta OD(t,\lambda)$ data must be time corrected. This is a crucial problem of the PSCP technique since the precision of this correction determines the final temporal resolution and photometric accuracy. We solved this problem in Ref. 18 using a nonresonant pump/probe signal from the pure solvent as a marker of zero delay for every probe wavelength. The pump/probe intensity cross correlation has FWHM$\approx$70 fs for every probe wavelength in the range 400–800 nm providing temporal resolution of 40 fs.

III. RESULTS

Representative kinetic traces of the pump/probe signal from LDS-750 in acetonitrile at 0.3 μJ pump energy are shown in Fig. 2. Two of them, (a and c), are given for the same wavelengths as in Ref. 7(a), allowing a direct comparison with data from fluorescence upconversion. The behavior of the signal at 654 nm [Fig. 2(a)] matches the corresponding

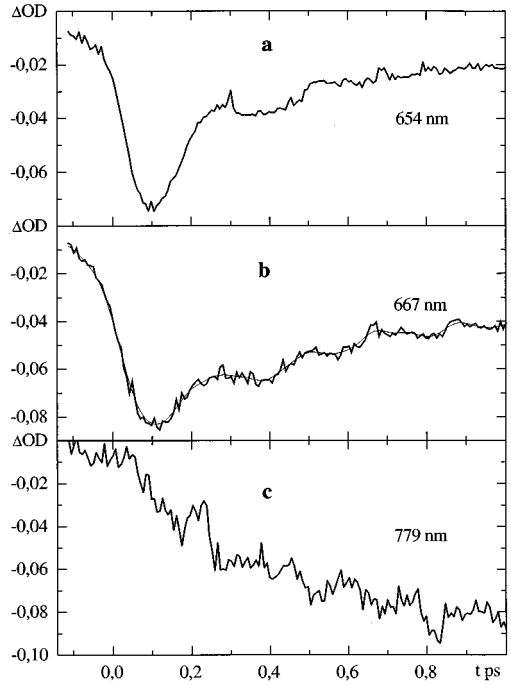

FIG. 2. Transient pump/probe signal at fixed wavelengths for LDS-750 in acetonitrile. The pump pulse of 0.3 μJ is centered at 530 nm. (a) 654 nm; (b) 667 nm; (c) 779 nm. The wavelengths in (a) and (c) are the same as in Ref. 7(a).

fluorescence trace. In addition we observe oscillations with a period of $\approx$200 fs (173 cm^{-1}) which are seen more prominently at 667 nm [Fig. 2(b)]. These oscillations are due to coherent excitation by the short pump pulse (resonant impulsive Raman process) of a low frequency optically active mode of the chromophore. They are detected because of shorter excitation pulses and better time resolution compared to Ref. 7(a). Since the oscillations persist on a 1 ps time scale, we assign them to the electronic ground state of LDS-750. The optical gain at 779 nm [Fig. 2(c)] is also similar to the corresponding fluorescence trace for the first 300 fs. Afterwards it continues to grow slowly while the fluorescence intensity remains nearly constant. The growth and decay of the fluorescence signal observed at 654 and 779 nm (after excitation at 608 nm) was attributed in Ref. 7(a) to ultrafast solvation. We show later that this interpretation is not compatible with the *whole* spectral evolution of the transient absorption and gain spectrum.[19]

Figure 3 shows time-corrected transient absorption and gain spectra of LDS-750 in acetonitrile for a pump pulse energy of 0.3 μJ. The upper panel gives the early spectral evolution from -98 to 70 fs in 14 fs steps. Negative ΔOD corresponds to bleaching or to stimulated emission, while a positive signal corresponds to transient absorption. Spectral structure is seen at the pump wavelength of 530 nm and prominently at 577 nm and at 670 nm. Weak shoulders can be discerned at 600 and 732 nm. The prominent bands appear at negative delay times, reach maximal contrast at zero delay and then disappear due to broadening after 70 fs.

The blue part of the spectrum at $\lambda < 530$ nm is dominated

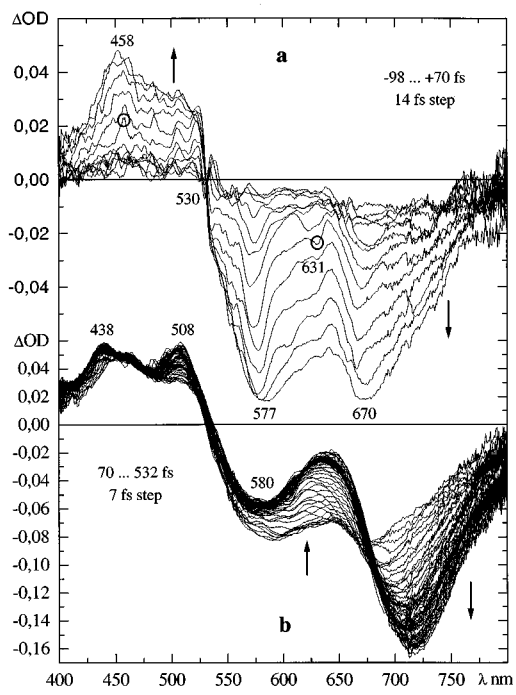

FIG. 3. Transient time-corrected pump/probe spectra of LDS-750 in acetonitrile at 22 °C, for excitation at 530 nm with 0.3 μJ pump pulse energy. Negative ΔOD corresponds to emission or bleaching and positive ΔOD to absorption. The evolution of the signal with increasing time is indicated by arrows (here and in Figs. 4–6). (a) Early spectral evolution from −98 to +70 fs in 14 fs steps. The time-zero spectrum is marked by circles at 458 and 631 nm (Raman scattering by the solvent; see the text). (b) Subsequent evolution from 70 to 532 fs in 7 fs steps. ΔOD decreases for $\lambda \geqslant 670$ nm because of stimulated emission; simultaneously ΔOD increases at shorter wavelengths. Light and dark regions correspond to fast and slow evolution, respectively.

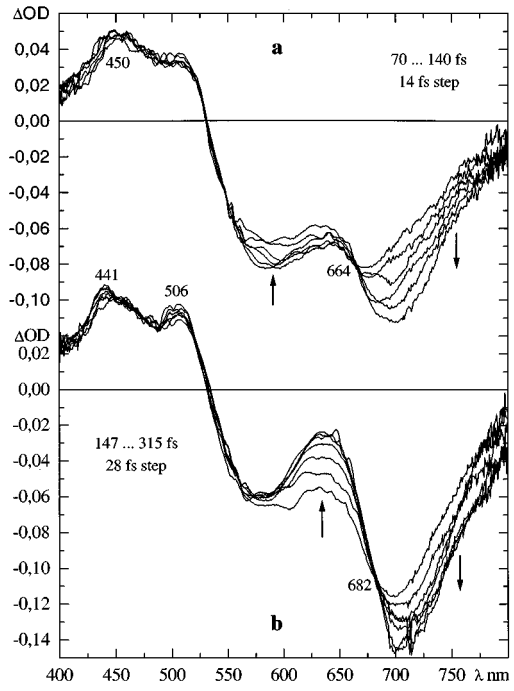

FIG. 4. Spectral evolution as in Fig. 2(b). (a) From 70 to 140 fs in 14 fs steps. A temporary isosbestic point is well defined at 664 nm. (b) From 147 to 315 fs in 28 fs steps. A second isosbestic point is located at 682 nm.

by excited-state absorption. A small peak at 458 nm corresponds to inverse stimulated Raman scattering by a CH stretching mode (2900 cm^{-1}) of pure acetonitrile. The same mode gives the stimulated Raman signal at 631 nm. The simultaneous growth and decay of these peaks provides a check on the experimental time correction which is better than ±15 fs.

The lower panel in Fig. 3 shows the spectral evolution from 70 to 532 fs in 7 fs steps. By comparison with the steady-state data, the broadband around 720 nm in the transient spectrum at 532 fs is readily identified with stimulated emission. Following the evolution from 70 fs to later times, ΔOD continues to decrease in the emission range 670–800 nm; simultaneously it increases in the range 550–670 nm (compare with Fig. 2). Light and dark regions correspond to fast and slow spectral evolution, respectively. It is particularly interesting that two isosbestic points are observed. The first, at 664 nm, is well defined from 70 to 140 fs. The second isosbestic point at 682 nm occurs during the interval from 140 to 315 fs. This is seen in Fig. 4 where the transient spectra for these time intervals are reproduced.

Figure 5 shows transient spectra after excitation with higher pump pulse energy of 1.2 μJ. In this case, we show later that excited-state $S_n \leftarrow S_1$ absorption of the pump pulse depletes the S_1 state which is afterwards repopulated by internal conversion. Optical gain develops around 720 nm with a risetime of 670 fs.

Figure 6 shows the spectral evolution in chloroform, a solvent of weaker polarity, for a pump pulse energy of 0.6 μJ. At early time two gain maxima at 577 and 700 nm are

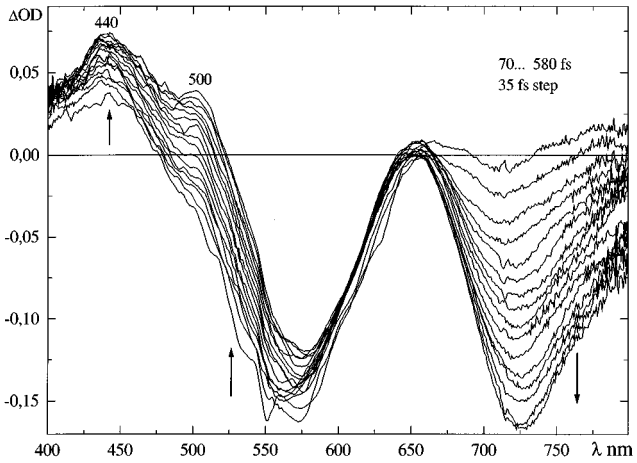

FIG. 5. Spectral evolution for higher pump energy of 1.2 μJ, from 70 to 580 fs in 35 fs steps. The stimulated emission contribution has its maximum around 720 nm and increases with time due to $S_n \rightarrow S_1''$ internal conversion (see Fig. 7). This process is also seen in the blue region by an increase of absorption there.

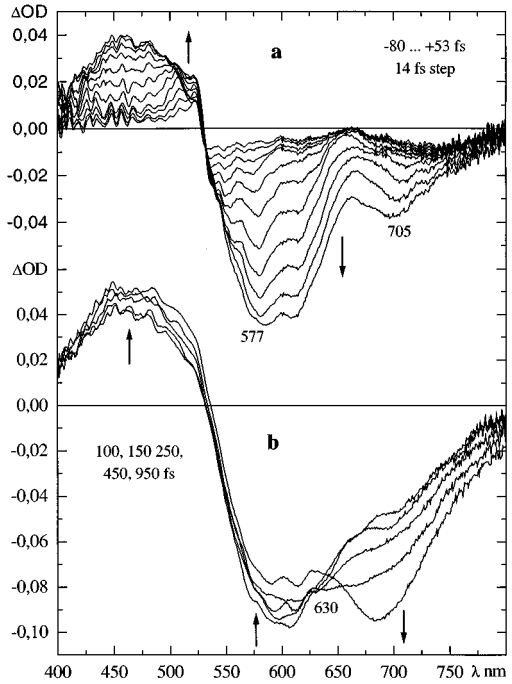

FIG. 6. Spectral evolution in chloroform solution for a pump energy of 0.6 μJ. (a) from -80 to 53 fs in 14 fs steps; (b) for 100, 150, 250, 450, and 950 fs.

clearly visible. At longer time the gain decreases around 600 nm and simultaneously increases at 700 nm. In general, the spectral evolution is slower, and there appears only one isosbestic region at 640 nm which is no longer well defined.

IV. DISCUSSION

A. Vibronic structure in the transient and steady-state spectra

We start our analysis with the acetonitrile dye solution. Consider first the transient spectral feature at 577 nm near the steady-state absorption maximum [cf. Fig. 3(a)]. At early time, while pump and probe pulses overlap, the transient signal consists in general of three components. The first is stimulated resonant Raman scattering of the pump at 530 nm. This coherent contribution should follow the pump/probe cross correlation. The other two components are due to the ''particle'' (population) in the excited state and to the corresponding ''hole'' (lack of population) in the ground state. Particle and hole are created by optical pumping at 530 nm, which selects chromophores with favorable solvent configurations for the interaction. Since the feature at 577 nm has maximal contrast at zero delay, we conclude that resonant Raman scattering makes the main contribution to the spectral structure. Its detuning from the pump frequency gives a frequency of $\approx$1500 cm^{-1} for the optically active vibration in the ground state.

This mode is also seen in the steady-state emission spectrum shown in Fig. 1. The entire emission spectrum (cross section σ_{em} for stimulated emission in the present case) is usually fitted to a log-normal distribution[22] over wave numbers $\tilde{\nu}$

$$f(\tilde{\nu})=\begin{cases} g_0 \exp\left\{-\ln(2)\left(\dfrac{\ln[1+2b(\tilde{\nu}-\tilde{\nu}_0)/\Delta]}{b}\right)^2\right\} & \text{if } 2b(\tilde{\nu}-\tilde{\nu}_0)/\Delta>-1 \\ 0 \quad \text{else} \end{cases}.$$

However, some vibronic structure is apparent as a red shoulder of the emission band of LDS-750. Therefore, the entire band is described by a sum of lognormal functions, each of which should account for a vibronic subband. We find that three functions are required for a fit to within experimental noise. With the asymmetry parameter b constrained to be equal for all components, the optimized parameters are $b=-0.242$ and $\tilde{\nu}_0$=14 098, 13 743, 12 236 cm^{-1}; Δ=1700, 1210, 1370 cm^{-1}; g_0=0.451, 0.587, 0.127 Å^2, respectively. The last two subbands are located at 727 and 817 nm, and they essentially describe the emission peak and the red shoulder. The dominant subband should represent the $0'\rightarrow 0''$ transition for emission from the fully relaxed chromophore in its excited state. The shoulder component is redshifted from the dominant subband by $\tilde{\nu}\approx$1500 cm^{-1}, and it is taken to represent the $0'\rightarrow 1''$ transition for a corresponding ground-state mode. Its relative amplitude gives the relative Franck–Condon factor FC($0'\rightarrow 1''$)/FC($0'\rightarrow 0''$). This in turn may be related to a dimensionless displacement ΔQ (which is the displacement between excited- and ground-state harmonic oscillator potentials along the corresponding vibrational coordinate, measured in units of the zero-point amplitude). We find $0.50\leqslant\Delta Q\leqslant 0.60$. To summarize, the relaxed emission spectrum has a simple vibronic structure and a narrow spectral width.

It is reasonable to assume that the mode which is active in emission is also active in absorption. The entire $S_1\leftarrow S_0$ absorption band may then be roughly simulated as is shown by the dashed line in Fig. 1. The extended shape of the absorption band requires that the (dimensionless) equilibrium position of the active mode in the excited state is displaced by 1.4 from that of the ground state. Separate mode displacements for absorption (1.4) and steady-state emission ($\sim$0.60) indicate that the primary excited electronic state relaxes to a final emitting state with a different geometry, i.e., to an electronically excited isomeric form of the molecule.

The estimated pattern of vibronic transitions for absorption is also shown in Fig. 1 as vertical lines with a length

proportional to its Franck–Condon (FC) factor. The active modes in the bare molecule are, of course, more numerous; however, they are dominated by the above-mentioned pattern as seen, for example, from jet spectra of isolated molecules of another styryl dye.[20(a)] For the simulation, we have therefore convoluted the ''stick'' spectrum with an appropriate line shape function which should roughly account for intramolecular spectral congestion and solvent broadening.[21] Comparison with the experimental absorption spectrum places the $0' \leftarrow 0''$ transition at 600 nm.

B. Vibrational relaxation of the FC state in S_1

The pump pulse at 530 nm (indicated by an arrow in Fig. 1) is seen to excite mostly the $1' \leftarrow 0''$ transition, creating a ''particle'' in the first active vibrational level of the primary excited electronic state. Now consider again the spectral feature at 577 nm and the shoulder at 600 nm in Fig. 3(a). There will also be a contribution in this region by a spectral hole, i.e., the bleached $0' \leftarrow 0''$ transition. No significant particle emission $1' \rightarrow 1''$ is expected here because of its small FC factor (based on a displacement of 1.4). At early time during optical pumping, when there is no appreciable relaxation, the Raman and hole contributions form the intense signal around 577 nm. The latter component diffuses on the time scale of the pump pulse duration as the ultrafast broadening of the subband shows [cf. Fig. 3(a)]. Examining the transient spectra around the pump wavelength also allows an estimate of the characteristic time of vibrational relaxation of the excited Franck–Condon state. Prior to relaxation there should be a considerable gain contribution from the $1' \rightarrow 0''$ transition. If the process takes place on a resolvable time scale, it should show up as a significant change of the transient absorption signal at 530 nm. However, the transient spectra in Fig. 3(b) are nearly constant in time at 530 nm. We conclude that vibrational relaxation is finished before 70 fs, in agreement with an estimate for a solute molecule of similar complexity.[9(a)] As a consequence, relaxation processes on a time scale of 70 fs or longer should depend on the excitation wavelength only insofar as the excess vibrational energy leads to an increase of vibrational temperature for the S_1 state.

C. Evidence for isomerization processes

Next we turn to the main point of this article, the evolution in the region of the steady-state emission band. The band at 670 nm, which is prominent at zero delay, loses its contrast with increasing delay time as the temporal overlap of the pump and probe pulses is decreased. This may indicate a coherent contribution for delay times $\leqslant$70 fs, but the detuning of $\approx$3900 cm^{-1} from the pump frequency is difficult to explain. Alternatively, the band may be due to stimulated emission by population in vibrational levels of S_1. Transitions are indeed expected in this region at 659 and 732 nm, and the gain spectrum should be as extended as the absorption spectrum. Instead the observed band is quite narrow, similar to the steady-state gain band. We conclude that a change of mode structure has occurred and assign the band to stimulated emission from a transient isomeric form of the molecule.

But when is this isomerization process completed, and at which point is solvation solely responsible for the spectral evolution? At a delay of 200 fs [Fig. 4(b)], the transient gain band is well defined and quite similar to the steady-state gain band. The entire transient spectrum at 200 fs may be fitted by ground-state bleaching, excited-state absorption, and gain bands. The latter is described by a lognormal curve[22] with the optimized parameters $\tilde{\nu}_0 = 14\,080$ cm^{-1}, $b = 0.1$ (asymmetry), and $\Delta = 1790$ cm^{-1} ($\approx$FWHM in this case). Compared with the steady-state band, the transient gain band at 200 fs is located at an energy higher by only 330 cm^{-1} and is broader by 300 cm^{-1} (FWHM). In the interval between 70 and 315 fs, the signal grows in the region of 670–800 nm and decreases around 550–670 nm with temporary isosbestic points at 664 and 682 nm (Fig. 4). Such behavior is a characteristic feature of intramolecular relaxation processes.

There are several explanations for the occurrence of an isosbestic point in transient optical spectra. First, two diabatic electronic states may contribute different spectra each of which changes only in relative amplitude because of population relaxation from one state to the other. The spectral shapes of both contributions remain constant and an isosbestic point occurs. Second, one adiabatic excited electronic state may undergo vibrational relaxation, isomerization or solvation which alters the shape, position, and oscillator strength (and hence the amplitude) of its spectral contribution. Under special conditions, the three parameters may vary in such a way that an isosbestic point is obtained. But as the signal decreases on one side of the isosbestic point and increases on the other with the same time constant, as seen in Fig. 4, this further requirement renders the entire set of conditions improbable. Third, because the emitting state S_1 contributes the difference between its absorption and gain to the total signal, an isosbestic point may be caused by internal conversion $S_n \rightarrow S_1$ from higher electronic states S_n. Let us discuss the last possibility in greater detail.

As is seen in Fig. 3, the total signal at the pump wavelength (530 nm), which is the sum of negative bleaching and positive excited-state absorption, is close to zero during the whole spectral evolution. Because the bleach signal is strong at this wavelength (see Fig. 1), so must be the excited state absorption. Sequential two-photon absorption of the pump pulse therefore causes a depopulation of the first excited electronic state S_1 and a corresponding population of higher excited states S_n at early time. Subsequent internal conversion $S_n \rightarrow S_1$ creates an additional transient component in the observed transient spectra. This relaxation is seen in Fig. 3(b) as a small growth of absorption for $\lambda < 530$ nm. Now consider the spectral evolution in the intermediate range 530–670 nm, and suppose that the S_1 excited state absorption cross section here is larger than the cross section for stimulated emission. After 70 fs the negative bleach signal is constant in time. On the other hand, the S_1 contribution to the transient spectra (presumed positive) should increase

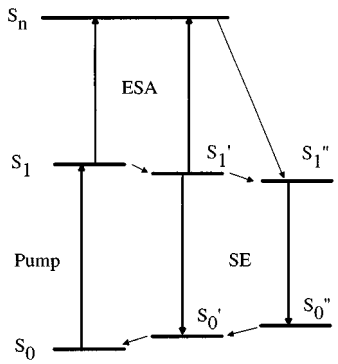

FIG. 7. Scheme of energy levels for LDS-750 and possible intramolecular relaxation pathways (thin arrows) after femtosecond excitation (see Sec. IV D).

with time due to $S_n \rightarrow S_1$ internal conversion and may thus cause the appearance of an isosbestic point.

We checked this explanation by studying the spectral evolution at a higher pump pulse energy (1.2 μJ). The results are shown in Fig. 5. From the preceding arguments we expect an enhancement of the spectral changes around the isosbestic points at 664 and 682 nm compared to the case of low excitation energy [Fig. 3(b)]. Instead, the transient spectra in Fig. 5 show only a small change in this region. Additionally, it can be inferred from the prolonged increase of absorption for $\lambda < 530$ nm, that the internal conversion process should show up as a corresponding significant increase also at low pump energy, whereas in fact the change in this region is small after 260 fs. Therefore, the explanation of the transient isosbestic points being caused by internal conversion should be ruled out. Moreover, the spectral evolution at higher pumping differs qualitatively from the one in Fig. 3(b), pointing at quite another aspect of the $S_n \rightarrow S_1$ internal conversion.

The first spectrum shown in Fig. 5 corresponds to a delay time of 70 fs. At this time, a broad background (ΔOD>0) in the red part is assigned to absorption both from S_1 and S_n. The last spectrum, at a delay of 580 fs, clearly shows the gain band which peaks around 725 nm. Retracing its evolution to earlier time, we observe a similar band even at 70 fs. The similarity strongly suggests that it also represents stimulated emission from the same emitting state. The spectral position at earliest time corresponds closely to that of the steady-state emission band, occurring higher in energy by just $\approx$170 cm^{-1}. It appears that the state which emits near the steady-state frequency—already then, at 70 fs and before—is created through an *intramolecular relaxation channel* which is accessed at higher excitation energy.

D. A model for the isomerization processes

A model for the different intramolecular relaxation processes is depicted in Fig. 7. Here, S_1 and S_1'' represent the initial, locally excited and the final emitting isomeric state, respectively. For 1.2 μJ pump energy, the initial population in S_n is high and comparable to that in S_1. Internal conversion from S_n populates *directly the final state* S_1'', but not S_1. The corresponding time constant is 670 fs in acetonitrile solution, as obtained from the growth of the optical gain. The internal conversion process is also seen in Fig. 5 as the growth of the absorption in the blue region, due to excited-state absorption from S_1''.

At low pump energy (0.3 μJ, Fig. 4), mainly the S_1 state is populated initially and the isomerization proceeds in two steps, $S_1 \rightarrow S_1' \rightarrow S_1''$. An intermediate isomeric state S_1' is associated with the early gain band at 670 nm; it may also be indicated by the first isosbestic point in the spectral evolution. The first step corresponds to the time interval 70–140 fs covered by Fig. 4(a), while the second step $S_1' \rightarrow S_1''$ is covered largely by Fig. 4(b). We estimate the averaged time constant for the isomerization as $\approx$200 fs. Note that some part of the change is still contributed by internal conversion from higher electronic states. The slow growth of the optical gain at 790 nm after 300 fs [Fig. 2(c)] may be attributed to this process.

For the chloroform solution, only one isosbestic point is observed. This may be explained by a close location of the S_1' and S_1'' energy levels. The pump energy of 0.6 μJ is intermediate between ''low'' and ''high'' pumping. Therefore, at early time [Fig. 6(a)], the transient emission band is peaked close to the stationary fluorescence maximum due to $S_n \rightarrow S_1''$ relaxation. At longer time the other relaxation channel $S_1 \rightarrow S_1''$ becomes dominant and reveals the isosbestic point. In general, the spectral evolution is similar in acetonitrile but slower, with a time constant of $\approx$600 fs.

The previous analysis shows that the ultrafast Stokes shift of the emission band in LDS-750 does not directly express ultrafast solvation as has been supposed before,[7] but that it is connected rather with some ultrafast conformational change of the chromophoric molecule. Still, the measured dependence of the isomerization rate on solvent polarity implies strong solute–solvent coupling and indicates that solvation may influence the isomerization process. As the main point of this paper, we emphasize that the transient spectral changes of LDS-750 should largely be considered intramolecular, while the dynamics may be composed of coupled intramolecular and solvation components.

Any further analysis must first describe the intramolecular isomerization process of LDS-750. The coordinates for this description are the dihedral angles for rotation around the single and double bonds of the central butadiene moiety, and for the rotation around the single bond linking the amino group to the chromophore. The identification of the reaction coordinate, or at least its qualitative assignment, may be possible by comparison with rigidized model derivatives where some coordinates are eliminated, or in systems which are otherwise restricted sterically. In the following we briefly point to molecular systems where this procedure has been applied, in order to find a case which best resembles that of LDS-750 so that some conjecture about the reaction coordinate for ultrafast photoisomerization of this dye in polar solvents can be made.

In a pioneering example, ultrafast transient absorption following fs excitation of bacteriorhodopsin[23] was explained by rotational isomerization of the retinal chromophore

around the bond between C_{13} and C_{14}, which is formally a double bond in the electronic ground state and changes to a single bond upon electronic excitation.[24] Yet the electronic structure of a polyene like retinal is quite different from that of styryl (better: hemicyanine) dyes like LDS-750, so that no conclusions regarding the latter may be drawn here. A model compound for intramolecular charge transfer (CT) in solution is *p*-dimethylamino benzonitrile (DMABN). The notion that charge transfer may be correlated with a rotation of the amino group into a perpendicular geometry relative to the benzonitrile moiety (twisted intramolecular charge transfer, TICT) was originally developed for this compound.[25] The characteristic time constant for the charge transfer process, of 20 ps in propanol, for example, was consequently assigned to rotational isomerization at the amino group.[26] This model has been juxtaposed by alternative explanations, like vibronic coupling between closely lying S_1 and S_2 (CT) states promoted by the inversion of the amino group,[27] or by charge transfer coupled to the CN bending coordinate.[28] So even in this generic case, the reaction coordinate has not been identified unequivocally. A clearer picture emerges of the photoinduced processes of styryl dyes like 4-dimethylamino-4′-cyanostilbene (DCS). In this case, bridged model derivatives showed that the amino group is *not* involved, and that the isomerization involves rotational changes around the single bonds between the phenyl rings and the ethylene moiety.[29] The fact that two single bonds are available for the process leads to rotational isomerism, which is avoided if no central ethylenic moiety is present. In this spirit, a simple hemicyanine dye was examined recently.[30] Here, the isomerization around the only central single bond involves large-amplitude motion, with a characteristic time constant of 25 ps in butanol; again amino group twisting could be excluded.

Let us return to LDS-750. Blanchard[31] proposed that the amino group rotates in the excited-state relaxation similarly to the TICT model for DMABN. In his picosecond pump/probe experiment, he described an inhomogeneous spectral relaxation for this dye in the slow solvent butanol. Using the phenomenological model of Agmon,[32] he calculated an isomerization time constant of 50 ps. The isomerization process which we observe is much faster, 200 and 600 fs for acetonitrile and chloroform solutions, respectively. Note that the other principal isomerization process, a conformational change of the central butadiene part (presumably involving double bonds[29]) which is responsible for fluorescence quenching, takes place with a time-constant of 160 ps in acetonitrile[16] and is therefore not important for our measurements. In view of the molecular systems mentioned in the previous paragraph, we conjecture that the ultrafast process observed by us involves rotations around the single bonds of the central butadiene moiety. If these angle changes are coupled, it is possible to construct a reaction coordinate which has low moment of inertia associated with it and small overall rotational amplitude. For forces similar to the model hemicyanine mentioned above,[30] the reduced effective mass and amplitude could speed up the process by more than an order of magnitude.

We should mention that the spectral evolution revealed in this experiment appears to be general for styryl dyes. Recently, we found a similar behavior for DCM[18] and DASPI[33] in a variety of solvents, and equivalent results have been obtained for DCS in acetonitrile and methanol.[20(b)] However, in view of the high dimensionality of the isomerization problem for these dyes, *conclusive* descriptions of the main geometry changes and the evolution of the adiabatic electronic states cannot be made at present.

V. CONCLUSION

Transient pump/supercontinuum probe spectra of the dye LDS-750 in polar solvents were recorded with 40 fs time resolution after ultrashort excitation at 530 nm. The results show that solvation is not directly connected with the transient Stokes shift of the emission band. At high pumping energy, the final emitting state is populated by internal conversion from higher electronic states S_n, and the subsequent dynamic Stokes shift of the emission band is negligible. The final excited state is therefore assigned to an isomeric form of the molecule with a similar dipole moment in its electronic excited and ground states, respectively. The same final excited state is normally reached from the first excited electronic state S_1 in an isomerization process, the characteristic time scale of which depends on solvent polarity. The nature and extent of this solvent dependence needs to be further clarified.

ACKNOWLEDGMENTS

We gratefully acknowledge financial support by the Max-Planck-Society, the Deutsche Forschungsgemeinschaft, and the Fonds der Chemischen Industrie.

[1] (a) P. F. Barbara and W. Jarzeba, Adv. Photochem. **15**, 1 (1990); (b) K. Yoshihara, K. Tominaga, and Y. Nagasawa, Bull. Chem. Soc. Jpn. **68**, 696 (1995).
[2] (a) M. Maroncelli, J. Chem. Phys. **94**, 2084 (1991); (b) M. Maroncelli, J. Mol. Liq. **57**, 1 (1993); (c) P. V. Kumar and M. Maroncelli, J. Chem. Phys. **103**, 3038 (1995).
[3] E. A. Carter and J. T. Hynes, J. Chem. Phys. **94**, 5961 (1991).
[4] (a) T. Fonseca and B. M. Ladanyi, J. Mol. Liq. **60**, 1 (1994); (b) T. Fonseca and B. M. Ladanyi, J. Phys. Chem. **95**, 2116 (1991).
[5] F. O. Raineri, H. Resat, B.-C. Perng, F. Hirata, and H. L. Friedman, J. Chem. Phys. **100**, 1477 (1994).
[6] B. M. Ladanyi and R. M. Stratt, J. Phys. Chem. **99**, 2502 (1995); *ibid.* **100**, 1266 (1996).
[7] (a) S. J. Rosenthal, X. Xie, M. Du, and G. R. Fleming, J. Chem. Phys. **95**, 4715 (1991); (b) M: Cho, S. J. Rosenthal, N. F. Scherer, L. D. Ziegler, and G. R. Fleming, *ibid.* **96**, 5033 (1992); (c) C.-K. Chan, S. J. Rosenthal, T. J. DiMagno, L. X.-Q. Chen, X. Xie, J. R. Norris, and G. R. Fleming, in *Dynamics and Mechanisms of Photoinduced Transfer and Related Phenomena*, edited by N. Mataga, T. Okada, and H. Masuhara (Elsevier Science, New York, 1992), p. 105.
[8] (a) S. J. Rosental, R. Jimenez, G. R. Fleming, P. V. Kumar, and M. Maroncelli, J. Mol. Liq. **60**, 25 (1994); (b) R. Jimenez, G. R. Fleming, P. V. Kumar, and M. Maroncelli, Nature (London) **369**, 471 (1994); (c) S. Vajda, R. Jimenez, S. J. Rosenthal, V. Fidler, and G. R. Fleming, J. Chem: Soc. Faraday Trans. **91**, 867 (1995).
[9] (a) M. L. Horng, J. A. Gardecki, A. Papazyan, and M. Maroncelli, J. Phys. Chem. **99**, 17311 (1995); (b) R. M. Stratt, M. Maroncelli, *ibid.* **100**, 12981 (1996).
[10] (a) T. Gustavsson, G. Baldacchino, J.-C. Mialocq, and S. Pommeret,

Chem. Phys. Lett. **236**, 587 (1995); (b) P. Hebert, G. Baldacchino, T. Gustavsson, and J.-C. Mialocq, *ibid.* **213**, 345 (1993).
[11] (a) H. Zhang, A. M. Jonkman, P. van der Meulen, and M. Glasbeek, Chem. Phys. Lett. **224**, 551 (1994); (b) P. van der Meulen, H. Zhang, A. M. Jonkman, and M. Glasbeek, J. Phys. Chem. **100**, 5367 (1996); (c) A. M. Jonkman, P. van der Meulen, H. Zhang, and M. Glasbeek, Chem. Phys. Lett. **256**, 21, (1996).
[12] D. Bingemann and N. P. Ernsting, J. Chem. Phys. **102**, 2691 (1995).
[13] (a) E. T. J. Nibbering, D. A. Wiersma, and K. Duppen, Chem. Phys. **183**, 167 (1994); (b) W. P. de Boeij, M. S. Pshenichnikov, and D. A. Wiersma, Chem. Phys. Lett. **247**, 264 (1995).
[14] T. Joo, Y. Jia, and G. R. Fleming, J. Chem. Phys. **102**, 4063 (1995).
[15] P. Vöhringer, D. C. Arnett, R. A. Westervelt, M. J. Feldstein, and N. F. Scherer, J. Chem. Phys. **102**, 4027 (1995)
[16] E. W. Castner, Jr., M. Maroncelli, and G. R. Fleming, J. Chem. Phys. **86**, 1090 (1986).
[17] G. J. Blanchard, J. Chem. Phys. **95**, 6317 (1991).
[18] S. A. Kovalenko, N. P. Ernsting, and J. Ruthmann, Chem. Phys. Lett. **258**, 445 (1996)
[19] Spectral reconstruction has been mentioned but not shown either in the communication [Ref. 7(a)] or in the regular article [Ref. 7(b)]. The spectral reconstruction in Ref. 7(c) is shown after normalization to a constant peak intensity; therefore important details of the spectral evolution are lost.
[20] (a) R. Daum, T. Hanson, R. Nörenberg, D. Schwarzer, and J. Schroeder, Chem. Phys. Lett. **246**, 607 (1995); (b) N. Eilers-König, T. Kühne, D. Schwarzer, P. Vöhringer, and J. Schroeder, *ibid.* **253**, 69 (1996).
[21] The centered line shape function [W. B. Bosma, Y. J. Yan, and S. Mukamel, Phys. Rev. A **42**, 6920 (1990)] for each vibronic transition is assumed to be composed of three components. Two strongly overdamped modes account for the solvent-induced broadening. Here, an estimated reorganization energy of 1500 cm^{-1} is partitioned according to the solvation correlation function for acetonitrile from Ref. 9(a) $\lambda_1=1029$ cm^{-1} with $\tau_1(=1/\Lambda_1)=89$ fs and $\lambda_2=471$ cm^{-1} with $\tau_2(=1/\Lambda_2)=0.63$ ps. The corresponding Δs are obtained in the high-temperature limit. The third mode accounts for spectral congestion, we set $\Delta_3=500$ cm^{-1} with $\lambda_3=0$ and $\Lambda_3\rightarrow 0$.
[22] D. B. Siano and D. E. Metzler, J. Chem. Phys. **51**, 1856 (1969).
[23] R. A. Mathies, C. H. Brito-Cruz, W. T. Pollard, and C. V. Shank, Science **240**, 777 (1988).
[24] W. T. Pollard, S.-Y. Lee, and R. A. Mathies, J. Chem. Phys. **92**, 4012 (1990), and references therein.
[25] (a) K. Rotkiewicz, K. H. Grellmann, and Z. R. Grabowski, Chem. Phys. Lett. **19**, 315 (1973); (b) Z. R. Grabowski, K. Rotkiewicz, A. Siemiarczuk, D. J. Cowley, and W. Baumann, Nouv. J. Chim. **3**, 443 (1979).
[26] Y. Wang and K. B. Eisenthal, J. Chem. Phys. **77**, 6076 (1982).
[27] K. A. Zachariasse, T. v. d. Haar, A. Hebecker, U. Leinhos, and W. Kühnle, Pure Appl. Chem. **65**, 1745 (1993).
[28] A. L. Sobolewski and W. Domcke, Chem. Phys. Lett. **259**, 119 (1996).
[29] (a) R. Lapouyade, K. Czeschka, W. Majenz, W. Rettig, E. Gilabert, and C. Rulliére, J. Phys. Chem. **96**, 9643 (1992); (b) W. Rettig, *Photoinduced Charge separation via Twisted Intramolecular Charge Transfer States*, in Topics in Current Chemistry, Vol. 169, Electron Transfer I, edited by J. Mattay (Springer, Berlin, 1994), p. 253.
[30] C. Röcker, A. Heilemann, and P. Fromherz, J. Phys. Chem. **100**, 12172 (1996), and references therein.
[31] G. J. Blanchard, J. Chem. Phys. **95**, 6317 (1991).
[32] N. Agmon, J. Phys. Chem. **94**, 2959 (1990).
[33] S. A. Kovalenko, J. Ruthmann, and N. P. Ernsting (in preparation).